23rd ABCM International Congress of Mechanical Engineering
December 6-11, 2015, Rio de Janeiro, RJ, Brazil

COMPARATIVE STUDY OF ROTOR ACTIVE VIBRATION CONTROL PERFORMANCE USING H_∞ AND μ-SYNTHESIS

Matheus Freire Wu
Ricardo Ugliara Mendes
Katia Lucchesi Cavalca
Laboratory of Rotating Machinery, Facuulty of Mechanical Engineering, University of Campinas, 200 Mendeleiev Street, 13083-970 Campinas, São Paulo, Brazil.
wu.matheus@gmail.com, rumqld@gmail.com, katia@fem.unicamp.br

Abstract. *Currently rotating machinery are largely used in many industrial sectors due to their broad range of applications, such as motors, turbines, compressors, and others. The growing demand for more efficiency requires faster, powerful and reliable rotors. Among the main obstacles that oppose the operation characteristics mentioned before are the vibrations associated to unbalance, that compromise the useful life of the mechanical system components. In order to reduce the undesirable vibration effects, there are different approaches, being one of them the active vibration control. There are distinct techniques and kinds of controllers available for this application, such as the well known PID (proportional differential integrative controller) which presents simplified mathematical model and good performance, but usually limited to simpler systems. For more complex applications, finding an acceptable PID tuning requires filters and different adaptations that demands a high experienced control designer. On the other hand, rotating machinery, in comparison to static structures, presents parameters that depend on the rotational speed, mainly the dynamic variation due to the gyroscopic effect and the stiffness and damping characteristics related to the oil film at the bearings. An alternative is to apply robust model based controllers, such as the H_∞ and μ-Synthesis. This kind of controller requires a more complex mathematical theory. However the final control design is relatively simple. It is known that a mathematical model can never perfectly describe a physical system, but robust controllers can sustain the systems stability and performance levels to acceptable levels even under uncertainty conditions. This paper aims to evaluate the application of robust controllers, H_∞ and μ-Synthesis, to control the vibration levels of rotating machinery, and their performance sensitivity regarding system's uncertainty.*

Keywords: *Rotor dynamics, Robust control, Vibration control*

1. INTRODUCTION

Rotating machinery are the basis of most industrial applications, as the productivity demand grows, faster, powerful and reliable machines are required. Conflicting with those objectives are unavoidable residual unbalanced mass, and components limitations causes the system to vibrate, creating an operational speed threshold and compromising mechanical parts.

Currently hydrodynamic bearing offers an interesting option as shaft support due to its high load, speed and damping capability, very low frictional coefficient, and theoretically infinity life spam. However there are some drawbacks, its dynamic coefficients are frequency dependent and they are the source of two self-excited phenomenon, oil-whirl and oil-whip. Oil-whirl usually occurs at half the rotational speed, depending on the situation it is negligible compared to unbalanced forces. When the rotational speed is twice a critical speed, oil-whirl matches the resonance frequency resulting in oil-whip effect, which causes strong vibration in the shaft, known as fluid-induced instability.

Aiming to reduce undesirable unbalanced vibrations, and more over, ensure stability at oil-whip frequencies, it is proposed to apply active control methods. There are many different approaches for this task. Maslen (2009) showed some of these possibilities applied to levitating magnetic bearings. In this work, two model based robust control techniques are compared, namely, H_∞ and μ-synthesis. The theory behind these kind of controllers may involve more complex algebraic work, but on the other hand it often provides more robust and better performance than the classical methods, such as the well known proportional integral differential controller (PID).

The controllers design are based on a finite elements model (FEM) of the rotor and required to stabilize it at a given frequency range, low rotational speed to above the fluid-induced frequency (twice the first critical speed). Both controllers performance are compared taking into account the resulting maximum singular value, the structured singular value (SSV), frequency and time response simulation.

2. MATERIALS AND METHODS

Design and comparison of the robust controllers are based on a FEM model of a rotor supported by two hydrodynamic bearings, which means its parameters are highly dependent on the operational speed. Since the main goal is to stabilize the oil-whip effect, the controllers should work properly from low speeds to above the instability speed (approximately 48Hz), so the operational range of analysis is settled from 15Hz to 48Hz. For the nominal plant, the model given at the rotation frequency of 30Hz is used as the base for the uncertain plant.

2.1 Rotor

The mechanical system used in this work consists in a horizontal SAE 1030 steel shaft, 800mm length and 12mm diameter, supported by two hydrodynamic bearings of 20mm width, 30mm inner diameter, and 90µm radial clearance, lubricated with ISO VG 32 oil, symmetrically positioned 600mm from each other. A steel disc, 47.5mm width and 95mm diameter is placed at the center of the shaft. The control force is exerted through a 80mm length and 40mm diameter, steel journal placed 62 mm from the second bearing (Figure 1). This rotor has its first flexional frequency at approximately 23Hz. Since this work is based only in simulations and focused on dealing with rotors' frequency dependency, the magnetic actuator model is not considered.

A FEM model of the rotor is created using 21 nodes with 4 degrees of freedom (DOF) each (two translations and two rotations) (Figure 1), according to Nelson and McVaugh (1976), cited by Mendes (2011), resulting in the movement equation Eq. (1). This model was validated in experimental tests by Mendes (2011). The resulting space-state model Eq. (2) has two times the total number of DOF (168 states), which would result in impractical order controllers. For that reason the system is divided in two parts, the first one includes the shaft, the disc and the journal, which parameters are not frequency dependent, and the second consists of the hydrodynamic bearings. This first system was reduced using the Guyan method (Guyan, 1964) (Eq.(3)) eliminating all nodes, except 3, 19, 11 and 16, corresponding respectively to bearing 1 and 2, the unbalanced mass and the control force input, which are the key nodes for the problem.

The reduced system presents the total of 16 DOF (in comparison to the original 84 DOF). With the reduced system, the bearings coefficients matrices, obtained by Machado e Cavalca (2009), according to Mendes (2011), are included at their respective nodes, resulting in a space-state equation with 32 states, preserving the first 16 modal frequencies.

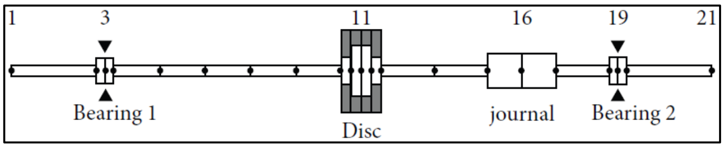

Figure 1. Rotor FEM model

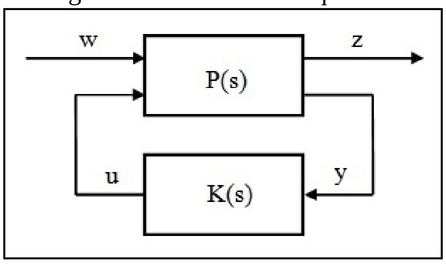

Figure 2. H∞ general problem

$$\boldsymbol{M\ddot{q} + (C + \Omega G)\dot{q} + Kq = F} \tag{1}$$

M, ***C***, ***K***, ***G***: Mass, damping, stiffness and gyroscopic matrix, respectively.
q, ***F***: DOF and external forces vectors, respectively.

$$\begin{cases} \boldsymbol{\dot{x} = Ax + Bf} \\ \boldsymbol{y = Cx + Df} \end{cases} \qquad \boldsymbol{A} = \begin{bmatrix} \boldsymbol{0} & \boldsymbol{I} \\ -\boldsymbol{M}^{-1}\boldsymbol{K} & -\boldsymbol{M}^{-1}\boldsymbol{C} \end{bmatrix} \tag{2}$$

x, ***y***, ***f***: States, output and input vectors, respectively.
B, ***C***: Zeros matrix with ones for input and output DOF, respectively.
D: Zeros matrix

$$\mathbf{M}_r = \mathbf{T}'\mathbf{MT} \quad \mathbf{C}_r = \mathbf{T}'\mathbf{CT} \quad \mathbf{K}_r = \mathbf{T}'\mathbf{KT} \quad \mathbf{G}_r = \mathbf{T}'\mathbf{GT} \tag{3}$$

$\boldsymbol{M_r}$, $\boldsymbol{C_r}$, $\boldsymbol{K_r}$, $\boldsymbol{G_r}$: Mass, damping, stiffness and gyroscopic reduced matrix, respectively.
T: Guyan reducing matrix.

2.2 Uncertainties

Performance and robustness of a controller are strong related to the mathematical model precision describing a real system. However its well known that it is impossible to perfectly describe all dynamic behaviors of a physical system. Besides, adding precision to the model usually result in a more complex mathematical solution, at some point it becomes impractical to work with. For that matter, a compromise between precision and simplicity is required. To deal with unmodelled, nonlinearities, and parameters imprecision of the model uncertainties can be added to the nominal system. There are many ways to describe uncertainties, some examples can be found at Zhou (1998), however, the larger the uncertainties boundaries, more conservative the controller has to be. That means, adding uncertainties does not replace a well defined nominal model.

In this work, parameters uncertainties are used. For the rotor model, it is supposed that the structure set without the bearings (which was previous labeled as the first part) has 5% uncertainty in its reduced stiffness matrix, and 10% at the reduced damping matrix. Another parameter included as uncertainty is the rotational speed range (15Hz to 48Hz). This uncertainty affects the system gyroscopic matrix and the bearings stiffness and damping matrixes. In this case, it is assumed that modeling errors for those parameters are negligible in comparison to the rotational speed effects.

2.3 H_∞ Control

The H_∞ design is a output feedback controller, within the so called modern control theory, which deals with non-linear, uncertain, and multiple inputs and outputs systems. First proposed by (Zames, 1981), the H_∞ controller aims to minimize the peak amplitude of the system's singular value diagram while ensuring robust stability, according to the small gains theorem, demonstrated in Zhou (1998), rejecting noises and disturbances. These characteristics makes the H_∞ control a very attractive option for rotor vibrations control application, since rotor models usually contains non-linear components approximations, are bound to disturbances and in practical situations it's not possible to acquire the full space-state vector. Moreover, reducing the system's infinity norm is directly related to attenuation in critical speed disturbances frequencies.

H_∞ general control problem can be described by the linear fractional transformation (LFT) block diagram in Figure 2, where the plant $\boldsymbol{P}$(s) (rotor transfer functions) has as inputs $\boldsymbol{w}$, representing the exogenous inputs (disturbances) and the control signal $\boldsymbol{u}$ (actuator forces), coming from the controller $\boldsymbol{K}$(s). As outputs there are the performance signals $\boldsymbol{z}$ (disc vibration and control effort) and feedback signals $\boldsymbol{y}$ (displacement at the bearings).

Figure 2 block diagram can be represented as the space state equations Eq. (4).

$$\begin{cases} \dot{x} = Ax + B_1 w + B_2 u \\ z = C_1 x + D_{11} w + D_{12} u \\ y = C_2 x + D_{21} w + D_{22} u \end{cases} \tag{4}$$

$\boldsymbol{x}$, $\boldsymbol{z}$, $\boldsymbol{y}$: States, performance and output vectors.
$\boldsymbol{A}$, $\boldsymbol{B_1}$, $\boldsymbol{B_2}$: Plant dynamic, exogenous inputs and control inputs matrices, respectively.
$\boldsymbol{C_1}$, $\boldsymbol{D_{11}}$, $\boldsymbol{D_{12}}$: Performance state, exogenous inputs and control signals components matrices, respectively.
$\boldsymbol{C_2}$, $\boldsymbol{D_{21}}$, $\boldsymbol{D_{22}}$: Output state, exogenous inputs and control signals components matrices, respectively.

Writing the space state system, in Eq. (4), as transfer functions results in Eq. (5):

$$\begin{bmatrix} \hat{z} \\ \hat{y} \end{bmatrix} = \begin{bmatrix} P_{11} & P_{12} \\ P_{21} & P_{22} \end{bmatrix} . \begin{bmatrix} \hat{w} \\ \hat{u} \end{bmatrix} \qquad \hat{u} = K(s)\hat{y} \tag{5}$$

$\hat{z}$, $\hat{y}$, $\hat{w}$ and $\hat{u}$, are the Laplace equivalent of $\boldsymbol{z}$ $\boldsymbol{y}$ $\boldsymbol{w}$ and $\boldsymbol{u}$ respectively.

Where,

$$\begin{cases} P_{11}(s) = C_1(Is - A)^{-1} B_1 + D_{11} \\ P_{12}(s) = C_1(Is - A)^{-1} B_2 + D_{12} \\ P_{21}(s) = C_{21}(Is - A)^{-1} B_1 + D_{21} \\ P_{22}(s) = C_2(Is - A)^{-1} B_2 + D_{22} \end{cases}$$

Writing the transfer function from inputs $\hat{w}$ to performance $\hat{z}$, Eq. (6)is obtained.

$$T(s) = P_{11} + P_{12} K(I - P_{22} K)^{-1} P_{21} \tag{6}$$

The H∞ problem consists in finding a controller $\boldsymbol{K}(s)$ that stabilizes the system and minimizes $\|\boldsymbol{T}(s)\|_\infty$. However, an optimum solution for $\boldsymbol{K}(s)$, with few exceptions, cannot be found, so usually an iterative solution is used to find a sub-optimum control such that $\|\boldsymbol{T}\|_\infty < \gamma$, for a given γ. Many different synthesis methods were developed since the H∞ problem was first formulated. In this work, the classical Riccati solution, formulated by Doyle et al. (1988) is applied and implemented by *Matlab® robust control toolbox*.

2.4 Weighting filters

Another important aspect of H∞ control regards to the weighting functions, which usually are simple gains or filters that shape the input and output signals. Weighting functions are included in the plant before determining the H∞ controller and have great influence above the final performance. Each filter has a different objective and effect, and they heavily depend on projects requirements. For that reason there is not an optimum value for then, but there are some directions that help finding acceptable parameters.

It's important to remark that a H∞ controller presents the same order as the plant transfer function, due to problems associated to high order models, which are very common concerning finite elements. However, applying simplifications and model reductions, such that only the most relevant parts are taken in account, makes the systems behavior outside of the frequency analysis range to be unknown. For this reason, in this project, the two most common filters $\boldsymbol{W_e}$ and $\boldsymbol{W_u}$ are applied (Figure 3). The weighting function $\boldsymbol{W_e}$ is a low-pass filter that actuates over the performance vector $\hat{z}$. The purpose is to attenuate disturbances in low frequencies and avoid higher frequencies where it would amplify disturbances effects in closed-loop. $\boldsymbol{W_u}$ is a high-pass filter that attenuates the control signal in frequencies higher than the model frequency range. It prevents the spill-off effect, mentioned in Sarracini (2006), which happens when high frequency components from the control signal excites natural modes not considered on the model. The weighting functions are given in Eq. (7) , given by Zhou (1998), which Bode magnitude diagrams as in Figure 4.

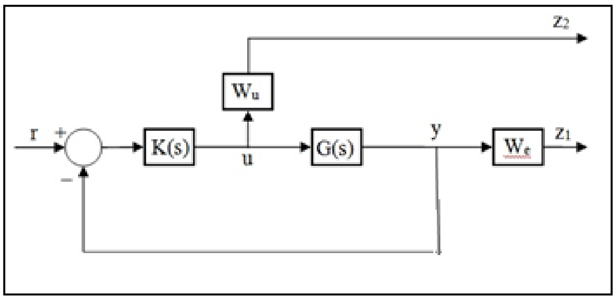

Figure 3. Weighting filters

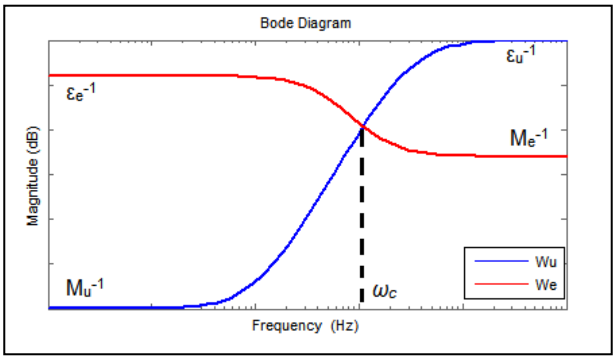

Figure 4. Weighting filters We e Wu sketch

$$W_e = \left(\frac{s / \sqrt[ke]{M_e} + \omega_c}{s + \omega_c \sqrt[ke]{\varepsilon_e}} \right)^{ke} \quad W_c = \left(\frac{s + \omega_c / \sqrt[ku]{M_u}}{s \sqrt[ke]{\varepsilon_c} + \omega_c} \right)^{kc} \tag{7}$$

M_e^{-1}, M_u^{-1}: stop band gain.
ε_e^{-1}, ε_u^{-1}: pass band gain.
ke, *ku*: filter order.
ω_c: cutoff frequency.

2.5 Singular structured value (μ)

An important analysis is to verify if stability is granted under the modeled uncertainty. A system's uncertainty can be "pulled out" (demonstrated in Zhou, 1998), resulting in the transfer function in Eq. (8), equivalent LFT in Figure 5, where ***M*** is the nominal system and $\mathit{\Delta}$ the normalized uncertainty matrix, ***g*** and ***h*** are respectively the output and input from Δ.

$$\begin{bmatrix} \boldsymbol{g} \\ \boldsymbol{z} \end{bmatrix} = \begin{bmatrix} \boldsymbol{M}_{11} & \boldsymbol{M}_{12} \\ \boldsymbol{M}_{21} & \boldsymbol{M}_{22} \end{bmatrix} \cdot \begin{bmatrix} \boldsymbol{h} \\ \boldsymbol{w} \end{bmatrix} \qquad (8)$$

$$\boldsymbol{h} = \Delta \boldsymbol{g}$$

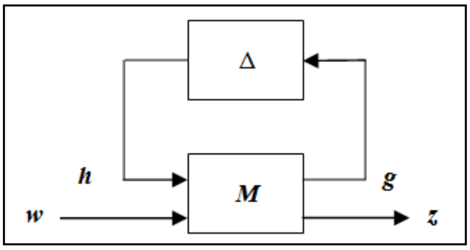

Figure 5. Uncertanties pulled out

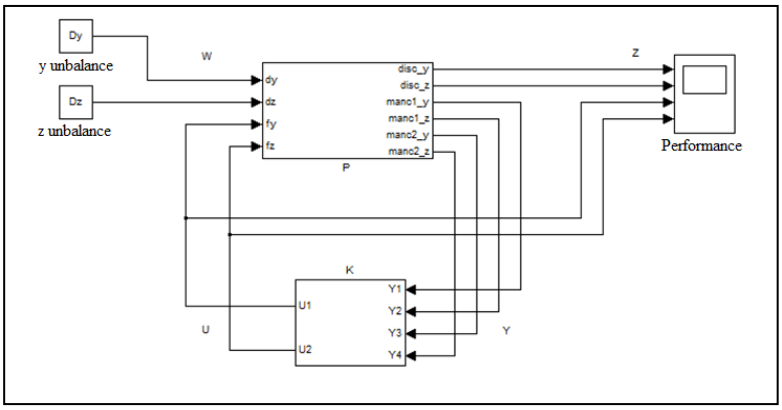

Figure 6. Closed loop block diagram

To guarantee stability and nominal performance, the respective conditions from Eq. (9) must be satisfied, which can be fulfilled by Eq. (10).

$$\begin{cases} \|\boldsymbol{M}_{11}\|_\infty < 1 \\ \|\boldsymbol{M}_{22}\|_\infty < 1 \end{cases} \qquad (9)$$

$$\|\boldsymbol{M}\|_\infty < 1 \Rightarrow \begin{cases} \|\boldsymbol{M}_{11}\|_\infty < 1 \\ \|\boldsymbol{M}_{22}\|_\infty < 1 \end{cases} \qquad (10)$$

Eq. (10) can even be written as an H_∞ control problem, however, as stated by Doyle et al.(1982), the analysis of $\|M\|_\infty$ is too conservative. Depending on Δ structure, only verifying the system's H_∞ norm can lead to the wrong conclusion about its stability. For that reason, Doyle introduced the so called singular structured value (SSV), denoted by μ. The SSV is a semi-norm that gives the inverse of the smallest $\|\Delta\|_\infty$ norm that destabilizes ***M***, defined by Eq. (11). Doyle defined the small μ theorem, or μ-analysis, similar to the well known small gain, in short it says that, iff $\|\boldsymbol{M}\|_\mu<1$, then the system ***M*** is stable for all the considered uncertainty Δ.

$$\|\boldsymbol{M}(j\omega)\|_\mu = \frac{1}{\min\{\bar{\sigma}(\Delta) : \Delta \in \mathit{\Delta}, \det(\boldsymbol{I} - \boldsymbol{M}\Delta) = 0\}} = \max_{\Delta \in \mathit{\Delta}} \rho(\boldsymbol{M}\Delta) \qquad (11)$$

$\boldsymbol{\mathit{\Delta}}$: is the set of Δ respecting the defined structure.

Calculating SSV usually cannot be done by algebraic methods, but Doyle proved that the μ-norm is bounded by the system spectral radius $\rho(\boldsymbol{M})$ and its maximum singular value $\bar{\sigma}(\boldsymbol{M})$, Eq. (12).

$$\rho(\boldsymbol{M}) \le \|\boldsymbol{M}\|_\mu \le \bar{\sigma}(\boldsymbol{M}) \qquad (12)$$

Knowing the bounds of μ-norm, it is possible to determine its value by maximizing the lower bound (ρ) and minimizing the upper bound ($\bar{\sigma}$). This procedure is done by finding some unitary transformation matrix ***D*** and applying it to the system, affecting both ρ and $\bar{\sigma}$, and defining a convex problem. However, it must be done for a determined frequency range, which may take some time, and does not guarantee to find the global maximum singular value.

2.6 μ-Synthesis controller

The μ-synthesis technique is based on the association of H_∞ control with the μ-analysis. As stated before, finding some controller ***K*** that reduces $\|\boldsymbol{M}\|_\infty$ is too conservative, but it is possible to minimize the Eq. (13), which is the upper bond of $\|\boldsymbol{M}\|_\mu$.

$$\inf_{\boldsymbol{K}}(\inf_{\boldsymbol{D}}(\boldsymbol{DM(K)D}^{-1})) \tag{13}$$

Looking at Eq. (13), it is clear that ***M*** depends on ***K***, ***D*** depends on ***M***(***K***), and so ***K*** depends on ***D***. Again it is not possible to find an optimum solution, but the iterative method *DK-iteration* proposed by Doyle (1985) leads to satisfactory results. It consists in calculating ***K*** for ***D***=***I***, then finding ***D***, using this last ***D*** to find a new ***K***, and so on. This method implemented by *Matlab® robust control toolbox*, usually converges in about 5 to 10 iterations, even though, complex plants, too much uncertainty parameters, and large frequency analysis range can make the process take quite a long time.

3. RESULTS

The final H_∞ controller is based on the reduced nominal model at the rotation frequency of 30Hz, and the μ-synthesis controller (denoted Kmu from now on) on the uncertain reduced nominal model. For comparison, the same weighting filters were applied to both controllers, the filters given in Eq. (7). Those filters were fitted by trial so that the system's H_∞ norm was reduced and the control signals were attenuated for frequencies higher than 100Hz, resulting in Eq. (14).

$$We = \frac{2.2s^2 + 4.976\cdot 10^4 s + 2.814\cdot 10^8}{s^2 + 2262s + 1.279\cdot 10^6} \quad Wu = \frac{0.022s^2 + 49.76s + 2.814\cdot 10^4}{10^{-3}s^2 + 71.53s + 1.279\cdot 10^6} \tag{14}$$

Both synthesized controllers presented high orders (H_∞ 40 and Kmu 48), using the balanced truncation method. These orders were reduced to 16 without sensitive performance loss. The closed loop for both controls follows the block diagram in Figure 6, linking the reduced controllers to the complete states plant.

3.1 μ-analysis

For stability tests the closed loop system were made using the reduced controllers linked to the full rotor uncertain model. Firstly and μ-analysis was made to verify if the closed loops were stable for the considered uncertainties. In Figure 7 and 8 the SSV is shown in the considered frequency for the full uncertain model without any control (G), the H_∞ closed loop (CL-Hinf) and Kmu closed loop (CL-Kmu). The important information here is if the SSV value goes beyond 1, which means instability. If the analyzed system is stable, the distance between the line peak and 1 gives the stability margin.

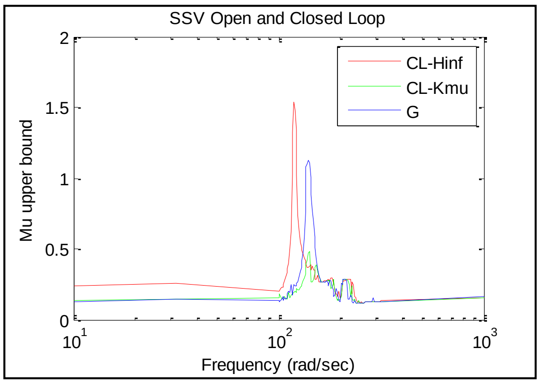

Figure 7. SSV plot

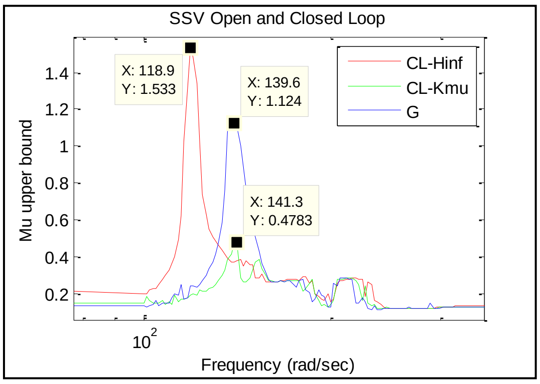

Figure 8. SSV plot (amplified view)

3.2 Maximum singular value analysis

Similar to Bode magnitude plot for singular input singular output (SISO) systems, the maximum singular value plot shows the system's maximum gain for combined input signals. Figures 9 and 10 shows the maximum singular value for nominal plant and closed loops (30Hz), and in Figures 11 and 12 sets (generated by arbitrary combinations of the uncertainties) for the uncontrolled plant (G) and closed loops (CL-Hinf) and (CL-Kmu).

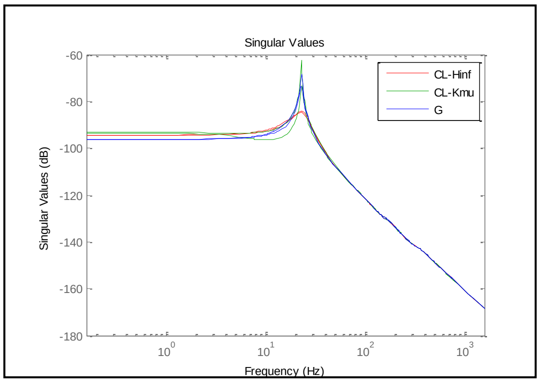

Figure 9. Nominal maximum singular value plot

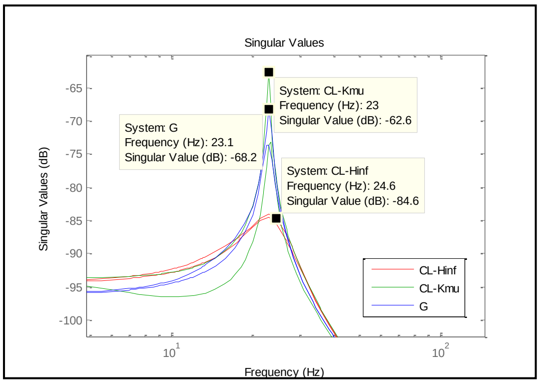

Figure 10. Nominal maximum singular value plot (amplified view)

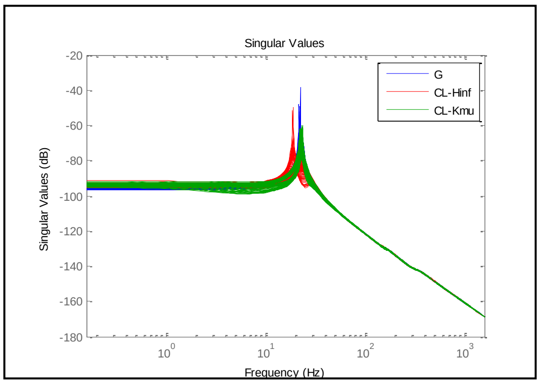

Figure 11. Sets of maximum singular value plot

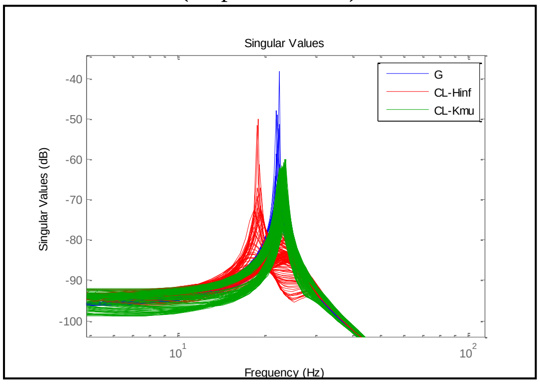

Figure 12. Sets of maximum singular value (amplified view)

3.3 Frequency and Time response analysis

Considering a residual mass unbalanced of 0.0395kg.m, the frequency response diagram was presented in Figure 13. The points at 42.66 Hz and 47.86 Hz are the stability limit for CL_Hinf and G respectively (CL_Kmu is stable up to approximately 140 Hz, not displayed in the diagram). Using *Simulink*®, the closed loop system from Figure 6 was simulated, having as inputs sinusoidal signals representing the unbalanced forces on the disc. Since the model changes according to the rotational speed, 3 tests were made (starting for zero initial conditions): for low frequency (15 Hz), critical speed (23 Hz) and above the instability frequency (48 Hz). Figures 14, 15 and 16 present the horizontal displacement response in time domain at the disc for the uncontrolled plant (G) and closed loops CL-hinf and CL-kmu for each rotational speed.

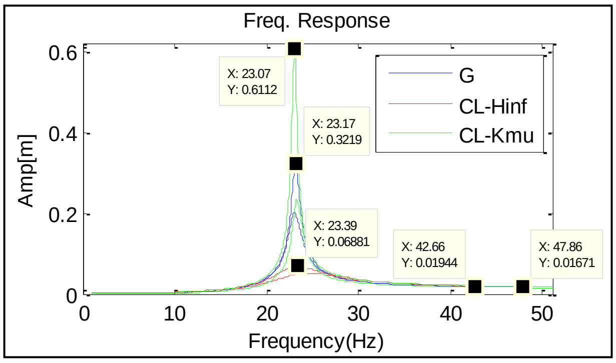

Figure 13. Frequency Response

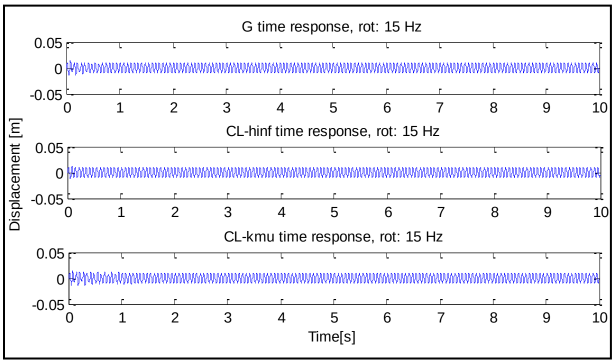

Figure 14. Horizontal time response at 15Hz

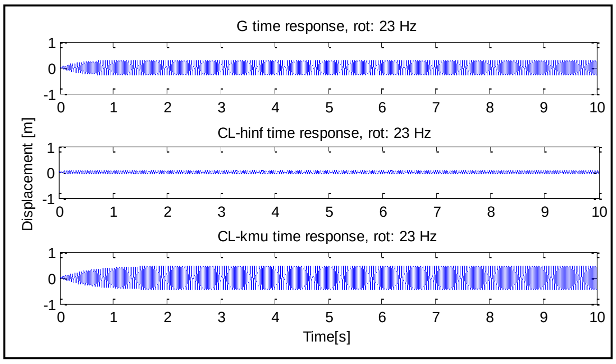

Figure 15. Horizontal time response at 23Hz

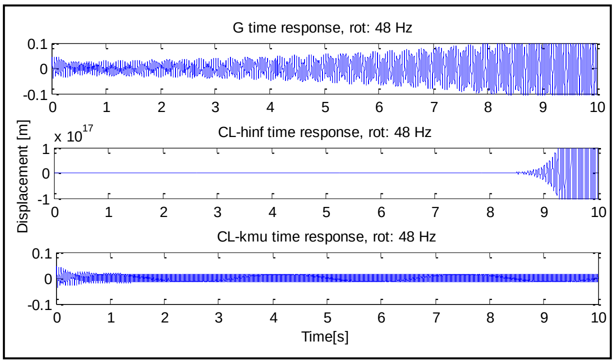

Figure 16. Horizontal time response at 48Hz

4. CONCLUSION

Analyzing the graphical results for μ-analysis (Figures 7 and 8) it is possible to conclude that the controller obtained by μ-synthesis method is capable of stabilizing all the considered uncertainties with a large margin, while H_∞ control, does not guarantee stability for the considered rotational speed range. On the other hand, the maximum singular value plots shows H_∞ offers considerable more attenuation near the critical speed (Figures 10, 13 and 15), but due to the lack of robustness this performance easily deteriorates in presence of uncertainties (Figure 11 and 12). Those conclusions can be confirmed through the time response plots (Figures 14, 15 and 16), which indicate the superior H_∞ attenuation near the critical speed, although the instability of the plant and the H_∞ for superior speeds, while the μ-synthesis controlled system maintains its stability.

Summarizing, the H_∞ may achieves better performances for nominal plants, but it's not suited for cases where there are considerable amount of parameter variation. Once in possession of a precise model and uncertainty bounds the μ-analysis provided a great tool for stability analysis. Moreover, it opened the possibility to μ-synthesis, which successfully stabilized the system for a large range of parametric variation, at the cost of deteriorating the response at the critical speed. It's important to remark that μ-norm requires iterative processes and, consequently, complex models can lead to substantially higher computer time costs.

In fact, none of the controllers alone presented an ideal solution. The most promising solution for this kind of problems seems to be adaptive controllers, since the parameters depends on the speed, which can be easily monitored. Some alternatives are: using switching method between the H_∞ and μ-synthesis depending on the speed; creating a scheduling control between various H_∞ ideal designed for small ranges of speed; or controllers based on parameter dependent Lyapunov equations.

5. REFERENCES

Doyle, J.C., Wall, J. and Stein, G., 1982. "Performance and robustness analysis for structured uncertainty." *IEEE Conference on Decision and Control*, pp. 629-636.

Doyle, J. D., 1985. "Structured Uncertainty in Control System Design." *IEEE Conference on Decision and Control*, pp. 260-265.

Doyle, J.D., Glover, K., Khargonekar, P. P. and Francis, B., 1988, "State-Space Solutions to Standard H_2 and H_∞ Control Problems." *IEEE American Control Conference*, pp. 1691-1696.

Guyan, R.J., 1964. "Reduction of Stiffness and Mass Matrices." *AIAA Journal*, v. 3, pp. 380.

Maslen, E. and Schweitzer, G., 2009. *Magnetic Bearings*. University of Virginia, Springer.

Mendes, R.U., 2011. *Desenvolvimento de Um Sistema de Atuação Magnética para Excitação de Sistemas Rotativos*. Thesis. Unicamp, Campinas.

Sarracini, F.J., 2006. *Síntese de Controladores H_∞ de Ordem Reduzida com Aplicações no Controle Ativo de Estruturas Flexíveis*. Thesis. Unicamp, Campinas.

Zames, G., 1981. "Feedback and Optimal Sensitivity: Model Reference Transformations, Multiplicative Semi-Norms, and Approximate Inverses." *IEEE Transaction on Automatic Control*, v. 26, pp. 301-320.

Zhou, K., 1998. *Essentials of Robust Control*, Prentice Hall.

6. RESPONSIBILITY NOTICE

The authors are the only responsible for the printed material included in this paper.